

# Infrared Radiation Coatings Fabricated by Plasma Spray

Xudong Cheng, Wei Duan, Wu Chen, Weiping Ye, Fang Mao, Fei Ye, and Qi Zhang

(Submitted August 21, 2008; in revised form March 21, 2009)

**Infrared radiation coatings were prepared by plasma spray on the copper sheet. The structure and emissivity were examined by x-ray diffraction and infrared radiant instrument, respectively. The results show that an appropriate addition of TiO<sub>2</sub> (5-15 wt.%) to NiO and Cr<sub>2</sub>O<sub>3</sub> leads to high emissivity of coating with (Cr<sub>0.88</sub>Ti<sub>0.12</sub>)<sub>2</sub>O<sub>3</sub> and NiCr<sub>2</sub>O<sub>4</sub> phase. However, more (20-30 wt.%) will frustrate the formation of NiCr<sub>2</sub>O<sub>4</sub> and ultimately decrease the emissivity. Moreover, the coating prepared by plasma spray endures a long working time without emissivity decrease.**

**Keywords** emissivity, infrared radiation coating, plasma spray

## 1. Introduction

Infrared radiation materials with high emissivity at high temperature have been widely used in many industrial applications such as energy savings for industrial furnaces (Ref 1-4), efficiency improvement of infrared heaters (Ref 5, 6), and spacecraft thermal control (Ref 7, 8). In these traditional applications, especially in industry furnaces, the infrared radiation materials, added with an amount of inorganic binder, were brushed onto the refractory furnace lining. The low adhesion strength between the coating and the metallic substrate and the bad thermal shock resistance restricted their application in the field of infrared radiation coatings of metal resistor tape, metal enclosures of hood-type annealing furnace, and others (Ref 9). Adhesion strength between the coating and the metallic substrate prepared by plasma spraying is much higher than one applied by the brush process obviously, because the plasma sprayed coating has a mechanical bond with the rough surface compared with the physical bond through the binder formed with the brush process. Plasma spray has been widely used in preparing wear-resistant coatings (Ref 10, 11), thermal barrier coatings (Ref 12, 13), abradable sealing coatings (Ref 14, 15), and so on. However, it is rare to find reports about preparing infrared radiation coating by plasma spraying. For this paper, the authors describe how they adopted plasma spraying to prepare infrared radiation coating.

Xudong Cheng, Wei Duan, Wu Chen, Weiping Ye, Fang Mao, Fei Ye, and Qi Zhang, State Key Laboratory of Advanced Technology for Materials Synthesis and Progressing, Wuhan University of Technology, Wuhan, China. Contact e-mails: xdcheng54@163.com and yluc@163.com.

Spinel structure materials are the first choice for application in middle- and high-temperature areas at present (Ref 16-18) because of their high emissivity in the whole band and great thermal stability under high vacuum and high temperature. In our experiment, spinel structure NiCr<sub>2</sub>O<sub>4</sub> is chosen as a basic material to study the structure and performance influence by the addition of TiO<sub>2</sub>.

## 2. Experimental

### 2.1 Preparation of Infrared Radiation Powders

In our experiment, the infrared radiation powders were fabricated by spray drying. Slurry was first acquired by mixing raw materials, organic binder, and deionized water in proportion. Agglomerated powder was prepared, in the spray dry tower, from well-ground slurry. The infrared emissivity of the materials is closely related to crystal structure. In order to obtain a high emissivity phase, the sample must be baked at 1200 °C before plasma spraying. Without such a process, materials obtained in spray dried powders where raw materials are only physically mixed cannot react sufficiently in plasma spraying with such limited time (less than 10<sup>-3</sup> s). After baking the powder and subsequently cooling in air, the sprayed powder was chosen from ones with 45-75 μm granularity. The composition of the raw materials is listed in Table 1.

### 2.2 Preparation of Infrared Radiation Coating

The preparation processes for infrared radiation coatings is similar to that for other wear-resistant coatings. In order to obtain well adhesion strength between coating and substrate, the pretreatment processes, such as cleaning, sandblasting, and preheating, were undertaken on the copper sheet. Prior to plasma spraying an infrared radiation coating, a Ni/Al bond coating was deposited on substrate. A homogeneous and dark infrared radiation coating was prepared on the pretreated copper sheet through GP-80 plasma spraying equipment.

**Table 1** Composition of infrared radiation materials (wt.%)

Sample	A	B	C	D
Cr <sub>2</sub> O <sub>3</sub>	68-72	60-67	49-56	85-90
NiO	29-32	25-29	21-24	...
TiO <sub>2</sub>	...	5-15	20-30	10-15

### 2.3 Characterization

The phase structures were identified from x-ray diffraction (XRD) patterns obtained using an x-ray diffractometer (Model D/MAXIII, Rigaku, Tokyo, Japan; 35 kV and 30 mA, monochromatic Cu K $\alpha$  radiation), at a scanning speed of 0.02°/s.

Relative infrared radiation energy is used in the experiment to measure the emissivity of the materials by obtaining the emissivity of the sample coatings from the radiant flux ratio of the coatings and blackbody at the same temperature. The measurement device (Model IRE-2) includes 6T61 infrared thermography, standard blackbody furnace, and sample heating furnace. The effective spectrum wavelength response of the 6T61 infrared thermography with mercury cadmium telluride (HgCdTe) infrared detector is within 1-21  $\mu\text{m}$ , which could cover the entire effective radiation range of the sample. In ordinary testing methods, the infrared light emitted from sample and blackbody are divided into several wave bands by spectrometer and the emissivities of each band are obtained, then the total emissivity is obtained by integrating the emissivity in the whole bands. However, in the authors' experiment, the normal total emissivities, both of the sample and blackbody, were measured in the whole bands by the width wave-band spectrum response detector without splitting the wave band.

## 3. Results and Discussion

### 3.1 Analysis of Structures

Figure 1 presents the XRD patterns of samples A, B, C, and D baked at 1200 °C. As shown in the figure, the baked sample A, without addition of TiO<sub>2</sub>, mainly consists of NiCr<sub>2</sub>O<sub>4</sub> and Cr<sub>2</sub>O<sub>3</sub> phase and does not contain NiO. This suggests that the adequate reaction between raw materials leads to the low or minimal content of NiO, which hence has no diffraction peaks.

When the amount of addition TiO<sub>2</sub> is 5-15% (sample B), (Cr<sub>0.88</sub>Ti<sub>0.12</sub>)<sub>2</sub>O<sub>3</sub> and NiCr<sub>2</sub>O<sub>4</sub> are the predominant phases. Because of the reaction between TiO<sub>2</sub> and part of Cr<sub>2</sub>O<sub>3</sub>, the lower content of Cr<sub>2</sub>O<sub>3</sub> leads to the lower content of reaction product NiCr<sub>2</sub>O<sub>4</sub> and hence the weaker diffraction peaks of spinel structure NiCr<sub>2</sub>O<sub>4</sub>. In addition, compared with diffraction peaks of Cr<sub>2</sub>O<sub>3</sub>, the peaks of (Cr<sub>0.88</sub>Ti<sub>0.12</sub>)<sub>2</sub>O<sub>3</sub> tend to have a slightly lower angle. This indicates an increase of interplanar distance of (Cr<sub>0.88</sub>Ti<sub>0.12</sub>)<sub>2</sub>O<sub>3</sub> compared with that of Cr<sub>2</sub>O<sub>3</sub> that results from Ti<sup>3+</sup> partly substituting for Cr<sup>3+</sup> in the Cr<sub>2</sub>O<sub>3</sub> crystal lattice; the Ti<sup>3+</sup> radius (0.76 Å) is slightly greater

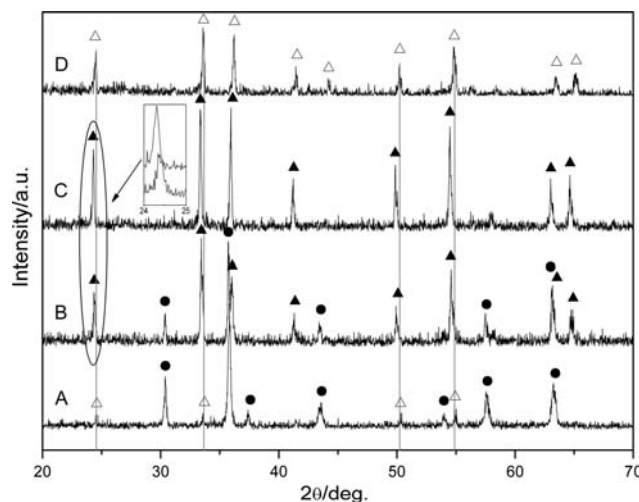


**Fig. 1** X-ray diffraction patterns of samples baked at 1200 °C. Open triangles, Cr<sub>2</sub>O<sub>3</sub>; closed triangles, (Cr<sub>0.88</sub>Ti<sub>0.12</sub>)<sub>2</sub>O<sub>3</sub>; closed circles, NiCr<sub>2</sub>O<sub>4</sub>

than Cr<sup>3+</sup> radius (0.69 Å), which increases the lattice so that the diffraction peak migrates slightly to the low angle, according to the Bragg equation.

When the amount of TiO<sub>2</sub> is up to 20-30% (sample C), the diffraction peaks of NiCr<sub>2</sub>O<sub>4</sub> disappear and only peaks of (Cr<sub>1-x</sub>Ti<sub>x</sub>)<sub>2</sub>O<sub>3</sub> were found. In addition, it is found in the amplification section from 24 to 25° that the diffraction peaks shift to the low angle according to the increase of the amount of TiO<sub>2</sub>. This suggests that with the increased amount of TiO<sub>2</sub>, more Ti<sup>3+</sup> enter into the Cr<sub>2</sub>O<sub>3</sub> crystal lattice to form (Cr<sub>1-x</sub>Ti<sub>x</sub>)<sub>2</sub>O<sub>3</sub> ( $x > 0.12$ ). Moreover, the larger amount of TiO<sub>2</sub> leads to a low content of Cr<sub>2</sub>O<sub>3</sub> reacting with NiO, and ultimately the diffraction peaks of NiCr<sub>2</sub>O<sub>4</sub> disappear.

As shown in the XRD patterns, no diffraction peaks of (Cr<sub>1-x</sub>Ti<sub>x</sub>)<sub>2</sub>O<sub>3</sub> were found in the baked powder sample D synthesized only from Cr<sub>2</sub>O<sub>3</sub> and TiO<sub>2</sub>. This indicates that the NiO plays an important role in formation of (Cr<sub>1-x</sub>Ti<sub>x</sub>)<sub>2</sub>O<sub>3</sub>.

### 3.2 Infrared Radiant Properties

It is true that the coating made up of NiCr<sub>2</sub>O<sub>4</sub> and Cr<sub>2</sub>O<sub>3</sub>, without the addition of TiO<sub>2</sub>, already has a high normal total emissivity up to 0.89 at 600 °C, because spinel structure materials have high emissivity in the whole band.

Furthermore, with 5-15% TiO<sub>2</sub> added into the raw material, the normal total emissivity of ultimate coating can increase even up to 0.91 at 600 °C. The structural reason for the increase is that when Ti<sup>3+</sup> is substituted partly for Cr<sup>3+</sup> in the Cr<sub>2</sub>O<sub>3</sub> lattice, the lattice distortion and reduction of crystal structure symmetry that enhance the vibration activity of lattice appear, ultimately, to promote launch and absorption of infrared radiation (Ref 19, 20).

However, when the amount of TiO<sub>2</sub> increases to 20-30%, the normal total emissivity of ultimate coating decreases to 0.89. Although Ti<sup>3+</sup> substitutes for more Cr<sup>3+</sup>

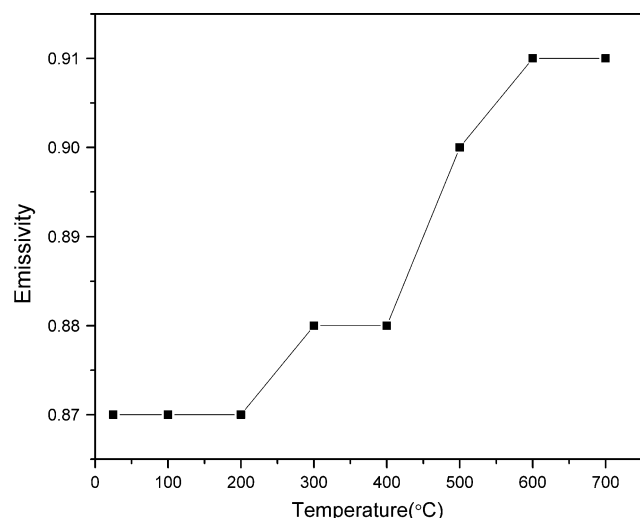


**Fig. 2** The relationship between emissivity and temperature

in the  $\text{Cr}_2\text{O}_3$  lattice to form  $(\text{Cr}_{1-x}\text{Ti}_x)_2\text{O}_3$  ( $x > 0.12$ ), which causes larger lattice distortion and favors enhanced infrared emissivity, the increased  $\text{TiO}_2$  hinders the formation of  $\text{NiCr}_2\text{O}_4$  and hence results in a decrease of emissivity. That explains the reason why emissivity decreases.

Without adding NiO, the normal total emissivity of the coating mainly made up of  $\text{Cr}_2\text{O}_3$  is only 0.86 at 600 °C.

In addition to the aforementioned experiment, coating B was chosen to undergo a test where emissivity varies with temperature (Fig. 2). The normal total emissivity is only 0.87 from room temperature to 200 °C, while with an increase in temperature the emissivity increases sharply and is 0.88, 0.9, and 0.91 at 200, 500, and 600 °C, respectively. When temperature increases to 700 °C, the coating emissivity still stays at 0.91.

After working 2000 h with vacuumity at  $1 \times 10^{-4}$  Pa and temperature at 600 °C, the emissivity remains 0.91 at 600 °C.

## 4. Conclusions

When the addition of  $\text{TiO}_2$  is 5-15%, the emissivity of coatings increase to a high value 0.91 at 600 °C; furthermore, they do not weaken after undergoing long working times. The high emissivity comes from the  $(\text{Cr}_{1-x}\text{Ti}_x)_2\text{O}_3$  and  $\text{NiCr}_2\text{O}_4$  phases existing in the coating.

## Acknowledgments

The authors would like to thank Yu Zeng and Ping Ye of China National Infrared & Industrial Electrothermal Products Quality Supervision & Testing Centre, for the

infrared normal total emissivity measurements of the coatings.

## References

1. I. Benko, High Infrared Emissivity Coating for Energy Conservation and Protection of Inner Surfaces in Furnaces, *Int. J. Global Energy Issues*, 2002, **17**(1-2), p 60-61
2. T. Kleeb and J. Olver, High-Emissivity Coatings for Energy Savings in Industrial Furnaces, *Ind. Heat.*, 2007, **74**(6), p 57-61
3. R. Scott and S.D. Cherico, High-Emissivity Coating Technology Improves Annealing Furnace Efficiency, *Iron Steel Technol.*, 2007, **4**(5), p 319-324
4. P.C. Sheil and T.R. Kleeb, High-Emissivity Coatings for Improved Performance of Electric Arc Furnaces, *Iron Steel Technol.*, 2006, **3**(2), p 49-53
5. B. Rousseau, M. Chabin, and P. Echegut, High Emissivity of a Rough  $\text{Pr}_2\text{NiO}_4$  Coating, *Appl. Phys. Lett.*, 2001, **79**(22), p 3633-3635
6. A. Makris, Function of Cermet Elements in Heat Treating Furnaces, *Ind. Heat.*, 1994, **61**(11), p 46-50
7. R.K. Bird, T.A. Wallace, and S.N. Sankaran, Development of Protective Coatings for High-Temperature Metallic Materials, *J. Spacecr. Rockets*, 2004, **41**(2), p 213-220
8. X. Jiang, M. Soltani, and D. Mishkinis, Development of  $\text{La}_{1-x}\text{Sr}_x\text{MnO}_3$  Thermochromic Coating for Smart Spacecraft Thermal Radiator Application, *Eur. Space Agency*, 2006, (616), p 6
9. S. Feng, X. Lu, and S. Xu, Research Status and Developing Trend of the Infrared Radiation Energy Saving Coatings Used at High Temperature, *Ind. Heat.*, 2007, **36**(1), p 10-15 (in Chinese)
10. W. Tian, Y. Wang, and Y. Yang, Fretting Wear Behavior of Conventional and Nanostructured  $\text{Al}_2\text{O}_3$ -13 wt.%  $\text{TiO}_2$  Coatings Fabricated by Plasma Spray, *Wear*, 2008, **265**(11-12), p 1700-1707
11. H.C. Cheng, Z.X. Li, and Y.W. Shi, Microstructure and Wear Resistance of  $\text{Al}_2\text{O}_3$ - $\text{TiB}_2$  Composite Coating Deposited by Axial Plasma Spraying, *Surf. Eng.*, 2008, **24**(6), p 452-457
12. G.M. Ingo and T.D. Caro, Chemical Aspects of Plasma Spraying of Zirconia-Based Thermal Barrier Coatings, *Acta Mater.*, 2008, **56**(18), p 5177-5187
13. T. Patterson, A. Leon, B. Jayaraj, J. Liu, and Y.H. Sohn, Thermal Cyclic Lifetime and Oxidation Behavior of Air Plasma Sprayed  $\text{CoNiCrAlY}$  Bond Coats for Thermal Barrier Coatings, *Surf. Coat. Technol.*, 2008, **203**(5), p 437-441
14. D. Sporer, A. Refke, M. Dratwinski, M. Dorfman, I. Giovannetti, M. Giannozzi, and M. Bigi, New High-Temperature Seal System for Increased Efficiency of Gas Turbines, *Seal. Technol.*, 2008, **2008**(10), p 9-11
15. H.I. Faraoun, T. Grosdidier, J.L. Seichepine, D. Goran, H. Aourag, C. Coddet, J. Zwick, and N. Hopkins, Improvement of Thermally Sprayed Abradable Coating by Microstructure Control, *Surf. Coat. Technol.*, 2006, **201**(6), p 2303-2312
16. X.D. Cheng, D.H. Li, and J.C. Wang, Preparation and Study on NiCr Spinel High Temperature IR Radiation Coatings Material, *Paint Coat. Ind.*, 2006, **36**(1), p 24-26 (in Chinese)
17. Q. Xu, W. Chen, and R.Z. Yuan, Microstructure and Infrared Emissivity at Normal Temperature in Transitional Metal Oxides System Ceramics, *J. Wuhan Univ. Technol. Mater. Sci. Ed.*, 2000, **15**(2), p 15-20
18. H. Zhang, X.Q. Wang, and F.P. Liao, et al., Preparation of Ni-Cr Composite Sol and Its Application in High Emissivity Coating, *J. Funct. Mater.*, 2007, **6**(38), p 898-901 (in Chinese)
19. H. Takashima, K. Matsubara, and Y. Nishimura, High Efficiency Infrared Radiant Using Transitional Element Oxide, *J. Ceram. Soc. Jpn.*, 1982, **90**(7), p 373-379
20. Y. Zhang and D.J. Wen, Relationship Between Infrared Radiation and Crystal Structure in Fe-Mn-Co-Cu-O Spinel, *Acta Metall. Sin.*, 2008, **21**(1), p 15-20